Accepted Manuscript

Optimization of novel benzofuro[3,2-*b*]pyridin-2(*1H*)-one derivatives as dual inhibitors of BTK and PI3Kδ

Linyi Liu, Xinyu Li, Yu Cheng, Lianjian Wang, Huizhu Yang, Jiurong Li, Siying He, shuangjie Wu, Qianqian Yin, Hua Xiang

PII: S0223-5234(18)31101-2

DOI: https://doi.org/10.1016/j.ejmech.2018.12.055

Reference: EJMECH 10989

To appear in: *European Journal of Medicinal Chemistry*

Received Date: 28 September 2018

Revised Date: 8 December 2018

Accepted Date: 22 December 2018

Please cite this article as: L. Liu, X. Li, Y. Cheng, L. Wang, H. Yang, J. Li, S. He, shuangjie Wu, Q. Yin, H. Xiang, Optimization of novel benzofuro[3,2-*b*]pyridin-2(*1H*)-one derivatives as dual inhibitors of BTK and PI3Kδ, *European Journal of Medicinal Chemistry* (2019), doi: https://doi.org/10.1016/j.ejmech.2018.12.055.

Exploreing the effect of different substituent group on activity

Exploreing the effect of aromatic heterocyclic ring on activity

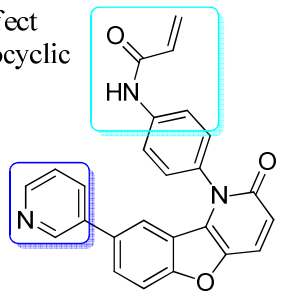

2

IC_{50} /BTK = 139 nM
IC_{50} /PI3Kδ= 275 nM
IC_{50}/Raji = 5.2 μM
IC_{50}/HL60 = 4.2 μM

This work

further optimization

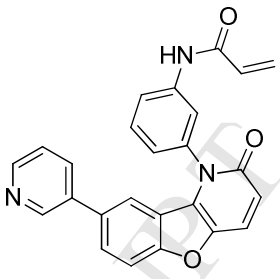

6f

IC_{50} /BTK = 74 nM
IC_{50} /PI3Kδ= 170 nM
IC_{50}/Raji = 2.1 μM
IC_{50}/Ramos = 2.65 μM

Optimization of novel benzofuro[3,2-*b*]pyridin-2(*1H*)-one derivatives as dual inhibitors of BTK and PI3Kδ

Linyi Liu[1,2,3]; Xinyu Li[1,2]; Yu Cheng[1,2]; Lianjian Wang[1,2]; Huizhu Yang[1,2]; Jiurong Li[1,2]; Siying He[1,2]; shuangjie Wu[2]; Qianqian Yin[3, **]; Hua Xiang[1,2, *,]

[1]Jiangsu Key Laboratory of Drug Design and Optimization, China Pharmaceutical University, 24 Tongjiaxiang, Nanjing 210009, China

[2]Department of Medicinal Chemistry, School of Pharmacy, China Pharmaceutical University, 24 Tongjiaxiang, Nanjing 210009, China

[3]Shanghai Institute for Advanced Immunochemical Studies, ShanghaiTech University, Pudong, Shanghai, 201210, China

[*]Corresponding author. Department of Medicinal Chemistry, School of Pharmacy, China Pharmaceutical University, 24 Tongjiaxiang, Nanjing 210009, PR China. Tel.: +86 025 83271096; Fax: +86 025 83271096. E-mail address: xianghua@cpu.edu.cn (H. Xiang).

[**]Corresponding author. E-mail address: yinqq@shanghaitech.edu.cn.

Abstract

BTK and PI3Kδ play crucial roles in the progression of leukemia, and studies confirmed that the dual inhibition against BTK and PI3Kδ could provide superior anticancer agents to single targeted therapies. Herein, a new series of novel benzofuro[3,2-*b*]pyridin-2(1*H*)-one derivatives were optimized based on a BTK/PI3Kδ inhibitor **2** designed by our group. Biological studies clarified that compound **6f** exhibited the most potent inhibitory activity (BTK: IC_{50} = 74 nM; PI3Kδ: IC_{50} = 170 nM) and better selectivity than **2**. Moreover, **6f** significantly inhibited the proliferation of Raji and Ramos cells with IC_{50} values of 2.1 μM and 2.65 μM respectively by blocking BTK and PI3K signaling pathways. In brief, **6f** possessed of the potency for further optimization as an anti-leukemic drug by inhibiting BTK and PI3Kδ kinase.

Keywords: Dual inhibitor; Oncology; B-cell malignancies; BTK; PI3Kδ.

1. Introduction

B cell receptor (BCR), a transmembrane receptor located on the cell surface of B lymphocytes, is essential for normal B-cell development and adaptive immunity [1,2]. However, aberrantly activated BCR signaling supports the survival and growth of malignant B cells [3]. Inhibition of BCR signaling has been used clinically to treat B-cell malignancies. These kinases such as LYN, SYK, BTK and PI3K in BCR pathway have become potential targets to develop kinase inhibitors for the treatment of B cell malignancies [4]. Among them, BTK and PI3K are gaining increasing attention as effective targets to develop therapeutic agents in clinic for the treatment of leukemia and lymphoma [5]. Ibrutinib as the first BTK inhibitor approved by FDA in 2013, exhibited significant clinical benefit in treating leukemia

and lymphoma, including chronic lymphocytic leukemia (CLL), mantle cell lymphoma (MCL), and Waldenström's macroglobulinemia (WM) [6]. Acalabrutinib, the second generation of BTK inhibitor, has been approved by FDA in 2017 for the treatment of MCL [7]. Meanwhile, PI3Kδ inhibitor idelalisib, the first approved PI3K inhibitor, has been applied to treat CLL and follicular lymphoma (FL) [8]. Recently, copanlisib, another PI3K inhibitor against PI3Kα and δ has been approved by FDA for the treatment of FL [9].

Unfortunately, acquired mutations has occurred frequently with single target drugs in disease progression and patients with drug resistance have a poor survival [11,12]. Nowadays, this drawback has been deemed to be overcome by multiple target drugs. On one hand, multiple target drugs could increase therapeutic effectiveness and keep cancer cells from developing resistance. On the other hand, they could also avoid the risks involved in multicomponent drugs or drug cocktails, such as poor patient compliance, unpredictable pharmacokinetic or pharmacodynamics profiles and drug−drug interactions [12,13]. In view of the cross-linking of BTK and PI3Kδ [14-16], the dual inhibition of BTK and PI3K is an attractive strategy to achieve more durable patient responses as well as preventing or delaying resistance [17,18]. Recently, Brahmam et al. reported a series of pyrazolopyrimidine derivatives as novel dual inhibitors of BTK and PI3Kδ. MDVN1003 [19] (**1**, Figure 1) which exhibited better oral bioavailability could reduce tumor growth in a B cell lymphoma xenograft model, and was more effective compared with either ibrutinib or idelalisib, although this compound showed relatively poor target selectivity [20]. Our group previously has reported a series of novel benzofuro[3,2-*b*]pyridine-2(*1H*)-one derivatives as BTK/PI3Kδ kinases inhibitors [21]. Further biological studies showed that compound **2** (Figure 1) exhibited better activities against BTK and PI3Kδ. Moreover, compound **2** significantly inhibited the growth of Raji cells and HL60 cells in vitro.

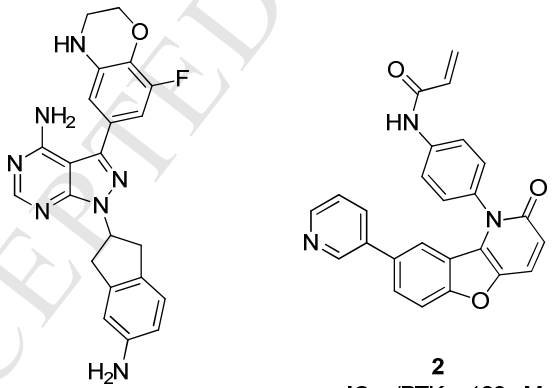

1 (MDVN1003)
IC_{50} /BTK= 32 nM
IC_{50} /PI3Kδ= 16 nM

2
IC_{50} /BTK = 139 nM
IC_{50} /PI3Kδ= 275 nM
IC_{50}/Raji = 5.2 μM
IC_{50}/HL60 = 4.2 μM

Figure 1. Synthesized BTK/PI3Kδ inhibitors.

According to the docking model of **2** with BTK and PI3Kδ (Figure S1) [21], we found that **2** occupied the ATP pocket of BTK and PI3Kδ, and its skeleton benzofuro[3,2-*b*]pyridin-2(1*H*)-one was extended towards the hinge region. Moreover, this binding mode exhibited two key hydrogen bonds: between the furan oxygen atom and MET477 of BTK as well as between the pyridine N and LYS799 of PI3Kδ. Nevertheless, the deficiency of interactions resulted in unsatisfactory activity compared with the lead compounds BTK inhibitor QL47 (**3**)

[22] and PI3K/mTOR inhibitor BEZ235 (**4**) [23] which both interact to BTK or PI3K with three different binding sites, respectively (Figure 2). These studies clarified compound **2** as a lead compound needs further optimization. Thus, we further designed and synthesized new benzofuro[3,2-*b*]pyridine-2(1*H*)-one derivatives to explore the structure-activity relationship and improve the biological activity based on the docking model of **2** (Figure 2).

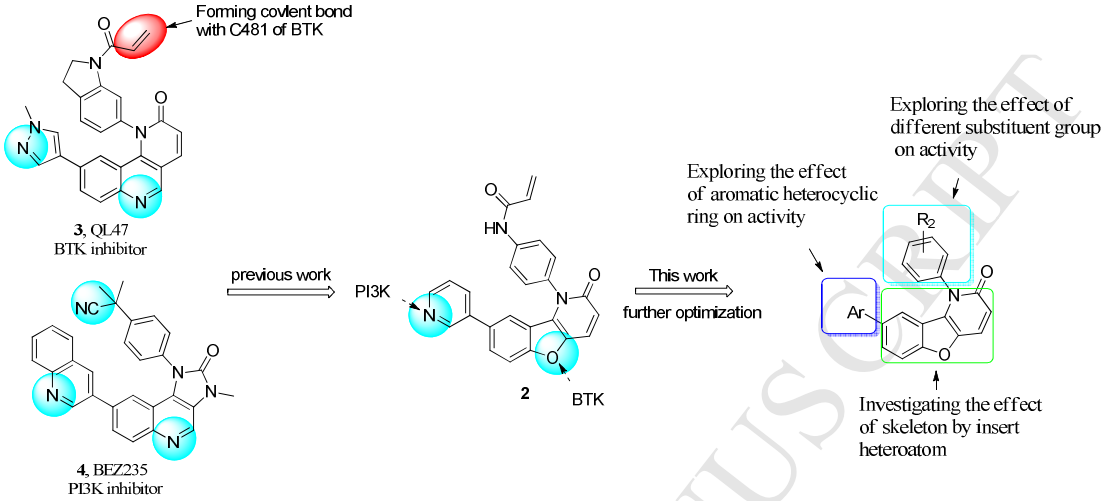

Figure 2. Optimization of **2** based on docking studies. Blue mark represents hydrogen bond receptor sites which form hydrogen bonds with residues of BTK or PI3K, while red mark represents covalent sites.

2. Results and discussion

2.1 Chemistry

The general reactions used for the synthesis of the novel targeted derivatives are outlined in Schemes 1~ 4. The starting material **S5**, 5-bromobenzofuran-3(2*H*)-one, was synthesized via several common reaction from methyl salicylate [20], and **S17**, 5-bromofuro[2,3-*b*]pyridin- 3(2*H*)-one, was synthesized from 2-hydroxynicotinic acid (Supplement information, Scheme 5). The furnished furan-3(2*H*)-one **S5** was subsequently condensated with *p*-nitroaniline, or *m*-nitroaniline affording intermediate **S6a** or **S6b** in a quantitative yield. Then, the key intermediate **S9a** or **S9b** was obtained through the acetylation, Vilsmeier-Haack cyclization and reduction reaction of **S6** continually with corresponding reagents as showed in Scheme 1. Further, the intermediate **S9a** was reacted with chloroacetyl chloride, closely following dimethylamine to provide the dimethylamine acetamide intermediate **S12** which was coupled with arylboronic acid to afford the final targeted benzofuro[3,2-*b*]pyridine-2(1*H*)-one derivatives **5a~5d** (Scheme 2). Meanwhile, **5e** was obtained from **5d** under the catalysis of trifluoroacetic acid. On the other hand, **S9a** was reacted subsequently with acryloyl chloride, and 2-fluoropyridine-5-boronic acid to provide acryloyl derivative **5f**.

In addition, the synthesis of final meta-substitutional derivatives **6a~6g** were performed as depicted in Scheme 3 when the amino was placed in meta-position. Amino derivative **S14** was obtained through the Suzuki coupling reaction of **S9b** with 2-methoxy-5-pyridineboronic acid. Then **S14** was reacted with chloroacetyl chloride, following appropriate aniline to provide alkylamino derivatives **6a~6d**. When acryloyl chloride was introduced into the compound **S9-B** firstly, the obtained intermediate **S16** was reacted with arylboronic acid to afford the target

molecules **6e~6g**.

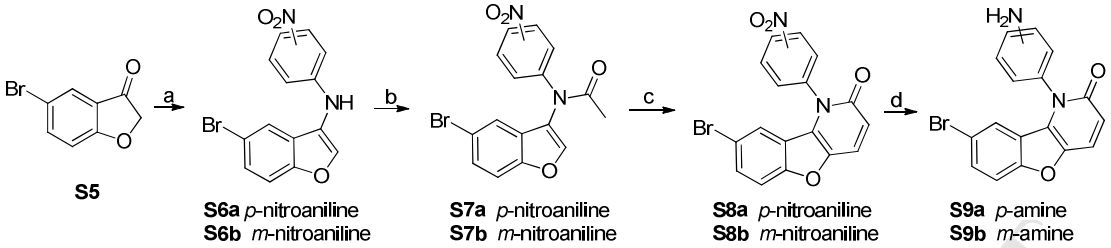

Scheme 1. Reagents and reaction conditions: a) *p*-nitroaniline, or *m*-nitroaniline, p-TSA, reflux, 100%; b) AcCl, NaH, 0 °C, 71%; c) $POCl_3$, DMF, 0 °C to 90 °C, 35%; d) Fe/NH_4Cl, reflux, 80%.

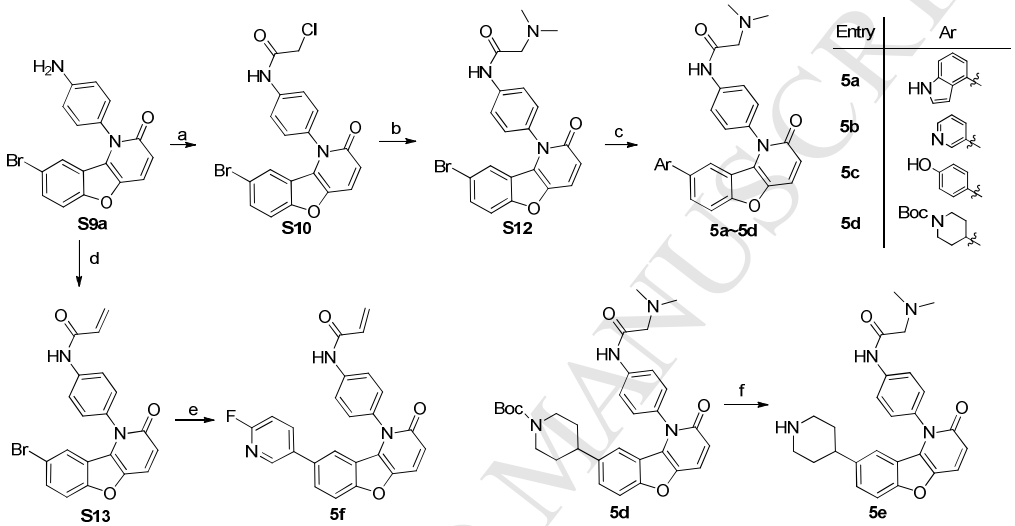

Scheme 2. Reaction conditions and reagents: a) Chloroacetyl chloride, K_2CO_3, DMF, 0 °C, 80%; b) Dimethylamine, K_2CO_3, KI, DMF, 60 °C, 70%; c) $ArB(OH)_2$, K_2CO_3, $Pd(PPh_3)_2Cl_2$, dioxane, 100 °C, 60%~80%; d) Acryloyl chloride, K_2CO_3, DMF, 0 °C, 80%; e) 2-fluoropyridine-5-boronic acid, K_2CO_3, $Pd(PPh_3)_2Cl_2$, dioxane, 100 °C, 60%~80%; f) Trifluoroacetic acid, DCM, 60%.

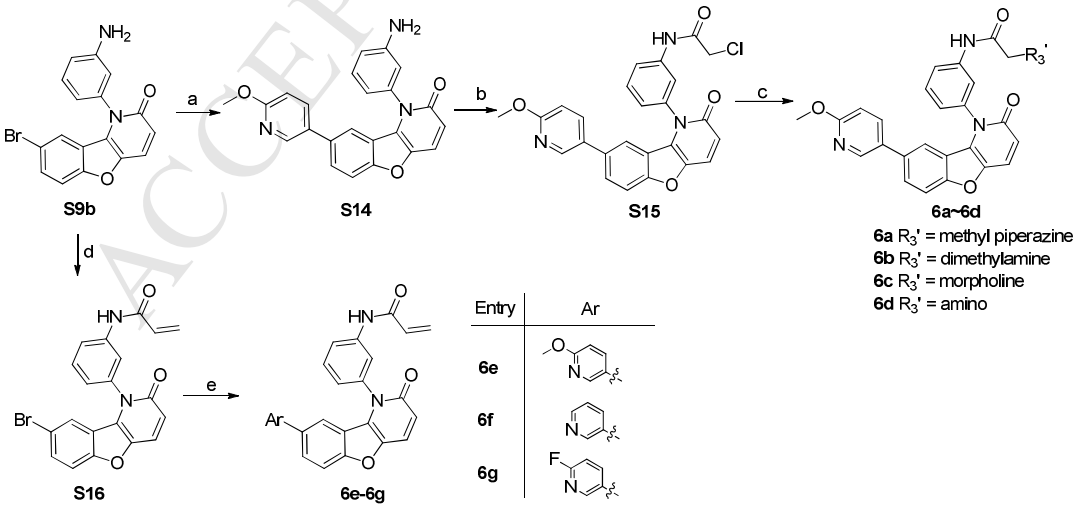

Scheme 3. Reaction conditions and reagents: a) 2-methoxy-5-pyridineboronic acid, K_2CO_3, $Pd(PPh_3)_2Cl_2$, dioxane, 100 °C, 80%; b) Chloroacetyl chloride, K_2CO_3, DMF, 0 °C, 75%; c) Appropriate aniline, K_2CO_3, KI, DMF, 60 °C, 60~90%; d) Acryloyl chloride, K_2CO_3, DMF, 0 °C,

80%; e) $ArB(OH)_2$, K_2CO_3, $Pd(PPh_3)_2Cl_2$, dioxane, 100 °C, 60%~80%.

Finally, the synthesis of final furo[2,3-*b*:4,5-*b'*]dipyridin-2(1*H*)-one derivatives **7a~7d** were prepared using the synthetic route showed in Scheme 4. The starting material **S17** was allowed to react with *p*-nitroaniline and acetylchloride to give acetamide intermediate **S19** which in turn was reacted with Vilsmeier-Haack reagent and Fe/NH_4Cl to afford the furo[2,3-*b*:4,5-*b'*] dipyridin-2(1*H*)-one intermediate **S21**. Next, several reactions were performed to give **7a~7d** derivatives through the coupling reaction and acylation reaction. At the end, all of the synthesized compounds have been confirmed by NMR and mass spectrometry.

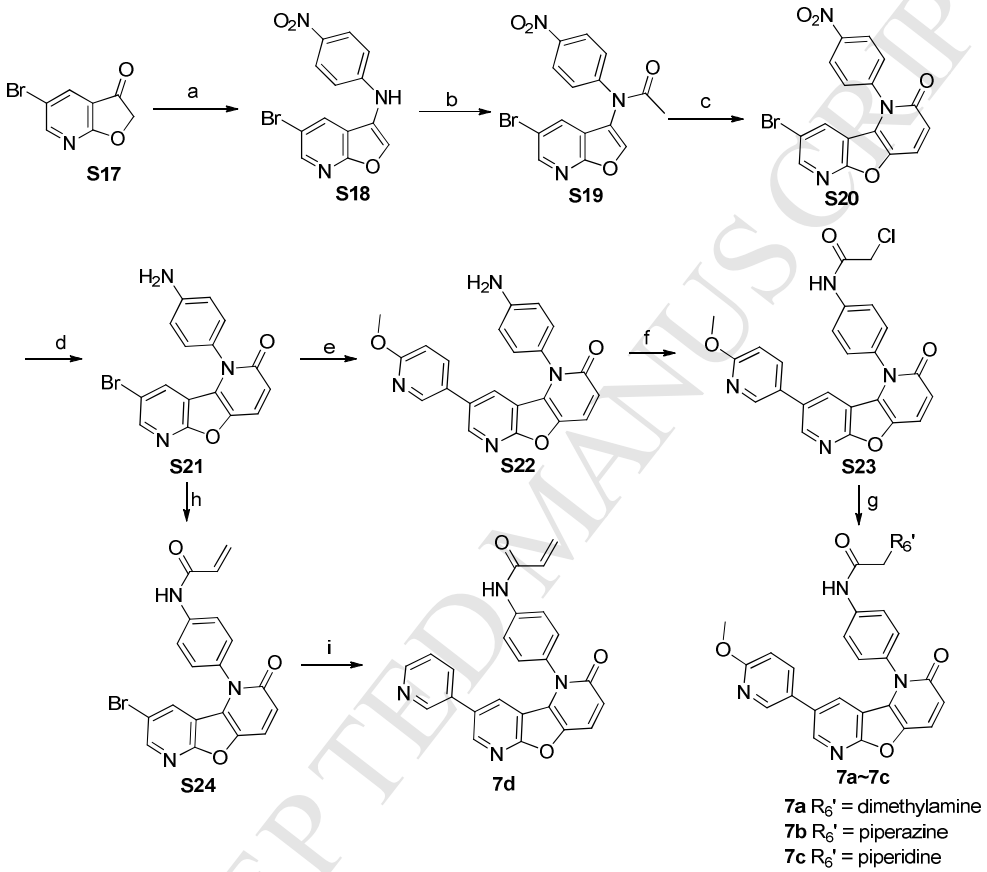

Scheme 4. Reaction conditions and reagents: a) *p*-nitroaniline, *p*-TSA, reflux, 100%; b) AcCl, NaH, 0 °C, 71%; c) $POCl_3$, DMF, 0 °C to 90 °C, 35%, d) Fe/NH_4Cl, reflux, 80%; e) 2-methoxy-5-pyridineboronic acid, K_2CO_3, $Pd(PPh_3)_2Cl_2$, dioxane, 100 °C, 80%; f) Chloroacetyl chloride, K_2CO_3, DMF, 0 °C, 70%; g) appropriate aniline, K_2CO_3, KI, DMF, 60 °C, 60~90%; h) Acyl chloride, K_2CO_3, DMF, 0 °C, 70%; i) 3-pyridylboronic acid, K_2CO_3, $Pd(PPh_3)_2Cl_2$, dioxane, 100 °C, 80%.

2.2 Biological activity

2.2.1 Anticancer activity and BTK, PI3Kδ assays

All these compounds were evaluated for their activity against BTK and PI3Kδ enzymes using ADP-Glo™ Kinase Assay. For comparison, BTK inhibitor ibrutinib and PI3K inhibitor BEZ235 were also tested as reference compounds. As shown in Table 1, these compounds effectively inhibited BTK with different levels at the concentrations of 200 nM, and part of them also

inhibited PI3Kδ. In particular, compound **6f** exhibited excellent inhibition with IC_{50} values of 74 nM against BTK and 170 nM against PI3Kδ, respectively. SAR analysis revealed that pyridyl substituent was significantly beneficial to anti-BTK activity, **5b** and **6f** possessed of better inhibitory activity, with IC_{50} values of 50 nM and 74 nM, respectively. Replacement of pyridyl substituent in **5b** with other heterocyclic groups or analogues yielded **5a** or **5c~e**, which were less potent than **5b** in inhibition of BTK. When attaching methoxy group to C-2 of pyridyl substituent in **6f**, the generated compound **6e** achieved an IC_{50} value of 0.08 nM in inhibition of BTK and exhibited similar inhibitory activity compared to **6f**. While introducing fluorine in pyridyl group, the inhibitory activities against BTK of compound **6g** declined significantly, indicating that the pyridyl group could achieve good potent BTK inhibitory activity while the stronger electron withdrawing group F was inappropriate to be installed on the C-2' position of pyridine. Furthermore, replacement of acrylamide group in **6e** with alkylamine generated **6a~6d**, which result in the decrease of inhibitory potency. This demonstrated locating the acrylamide group at meta-position of phenyl ring was beneficial for efficient inhibition against BTK. Actually, the acrylamide group was also beneficial to anti-PI3Kδ activity, these acryloyl analogues **5f**, **6e**, **6f**, **6g** and **7d** exhibited different PI3Kδ inhibitory activity. However, alkyl amino substituents, such as dimethylamino (**5b**), morpholine (**6c**) and piperidine (**7c**), were unfavorable to anti-PI3Kδ activity. The introduction of N at C-6 position (derivatives **7a-~7d**) did not improve the inhibitory activity of these analogs towards either BTK or PI3Kδ as depicted in Table 1, indicating the N atom was inappropriate to be installed here.

Based on the encouraging enzymes inhibitory activities of the newly synthesized analogs, the anticancer activity in vitro of these analogs was assessed using two typical B cell lymphoblastic leukemic cell lines Raji (Burkitt's lymphoma cell) and Ramos (Burkitt's lymphoma cell). These cell lines were chosen because they both express BTK and PI3K. The results were summarized in Table 1. The tested compounds showed variable anticancer activities against these two cell lines. Compound **6f** which showed the most dual potency against BTK and PI3Kδ exhibited slightly stronger inhibitory activity against Raji (IC_{50} = 2.1 μM) and Ramos (IC_{50} = 2.65 μM) cells. Furo[2,3-*b*:4,5-*b'*]dipyridin-2(1*H*)-one derivatives **7a~7c** showed minimal activity in Raji cells, indicating that the introduction of N at C-6 position adversely affected antiproliferative activity. These data taken together showed that this new series of furo[3,2-b]pyridine derivatives inhibited B-cell lymphoblastic leukemic cells by serving as potent dual inhibitors of BTK and PI3Kδ, and compound **6f** was an effective agent with anti-lymphoma cell activity.

Table 1. Effect of compounds on BTK, PI3Kδ and the cell viability of B cells: Raji and Ramos cell lines.

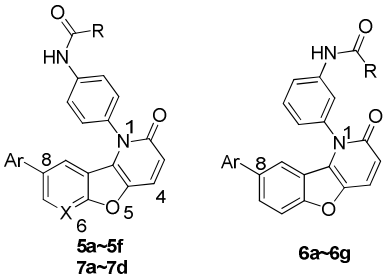

Entry	Ar	R	X	BTK		PI3Kδ		Anticancer activity IC_{50}/μM	
				Inh%/200 nM	IC_{50}/μM	Inh%/200 nM	IC_{50}/μM	Raji	Ramos
5a			C	47.2±2.9	-	NI	-	18.8	-
5b			C	63.4±1.3	0.050	NI	-	7.1	3.43
5c			C	51.7±5.4	0.150	NI	-	1.8	-
5d	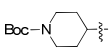		C	49.2±2.1	-	NI	-	7.0	-
5e			C	33.1±4.8	-	NI	-	2.4	-
5f	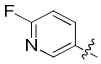		C	32.1±4.1	-	31.7±3.1	1.27	7.3	1.65
6a		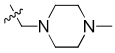	C	51.4±0.7	0.153	NI	-	18.0	-
6b			C	55±0.1	0.119	NI	-	7.2	-
6c		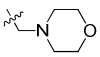	C	37.6±0.7	-	NI	-	>40	-
6d			C	19±0.1	-	NI	-	20.8	-
6e			C	67.3±2.6	0.08	11.3±3.0	-	2.4	1.3
6f			C	86.8±1.3	0.074	58.1±1.4	0.17	2.1	2.65
6g			C	40.2±4.1	0.55	34.0±2.9	0.92	2.2	1.86
7a			N	58.8±1.9	0.150	NI	-	>40	-
7b		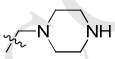	N	32±4.2	-	NI	-	33.7	-
7c		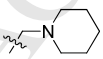	N	55±2.0	0.125	NI	-	>40	-
7d			N	38.7±5.5	-	34.2±3.9	1.0	7.4	1.33
ibrutinib				-	0.0007	-	-	14.5	5.8
BEZ235				-	-	-	0.022	0.22	0.0068

NI: no inhibition

2.2.2 Effect of **6f** on Raji cell viability

As shown in Table 1, compound **6f** exhibited the most potent biological activity, thus we

further investigated the effect of **6f** on cell viability of Raji cells. As depicted in Figure 3, ibrutinib didn't significantly inhibit the growth of Raji cells at the concentration of 5 μM before 24h, but induced substantial suppression of cell viability after 24h and reached the maximum inhibition after 48h. In addition, PI3K inhibitor BEZ235 exhibited a rapid and robust anti-proliferative effect on Raji cells at 5 μM, superior to that of ibrutinib. Importantly, **6f** displayed superior potency to that of ibrutinib or BEZ235 with more rapid suppressive effect. This result indicated that **6f** could significantly suppress the growth of Raji cells in time-dependent manner.

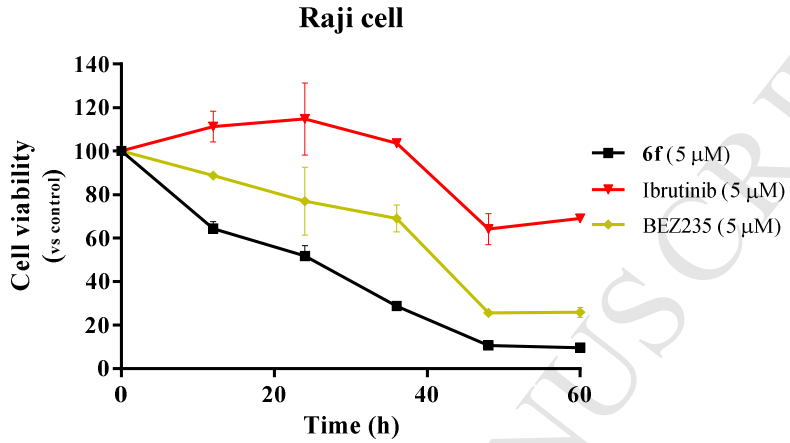

Figure 3. Effect of compounds on the temporal dependence of Raji cells viability

2.2.3 Selectivity of **6f** on PI3K isoforms and mTOR

Based on its impressive dual BTK/PI3Kδ kinase inhibitory activity and anti-proliferative effects, compound **6f** was selected for further study. It's known that BEZ235 is a pan inhibitor of PI3K and mTOR (the key kinase downstream of PI3K), so the selectivity of compound **6f** was evaluated against PI3K isoforms including PI3Kα, PI3Kβ, PI3Kγ as well as mTOR. The results in Table 2 showed that **6f** was less potent than BEZ235 against PI3K. Nevertheless, 6f displayed more potent inhibition and higher selectivity to PI3Kδ compared with compound **2**. Moreover, **6f** didn't inhibit mTOR but compound **2** has IC_{50} value of 228 nM. These data demonstrated that shifting the acryloyl group in compound **2** to meta-position was a reasonable optimization.

Table 2. Selectivity of **6f** to PI3K isoforms and mTOR

	IC_{50} /nM				
Entry	PI3Kδ	PI3Kα	PI3Kβ	PI3Kγ	mTOR
6f	170	855	2821	2183	>10000
2	275	254	838	684	228
BEZ235*	7	4	75	5	6

* Data from reference [21].

2.2.4 Effect of **6f** on BTK and PI3K mediated signaling pathway

In addition, the effect of **6f** on BTK and PI3K mediated signaling pathways in Ramos cells was further studied (Figure 4). The phosphorylation of BTK^{Tyr223} and its downstream signaling factor PLCγ-2 was significantly up-regulated under anti-IgM stimulation, but were inhibited substantially in concentration-dependent way following the treatment of **6f** or ibrutinib (Figure 4a). In addition, **6f** also blocked PI3K pathway (Figure 4b). The phosphorylation of Ser473 of Akt and

Ser2481 of mTOR was inhibited with the **6f** treatment, although the inhibitory activity is weaker than BEZ235. All the result clarified that **6f** could effectively block the BCR signaling by through inhibiting BTK and PI3K signaling pathway, thereby suppressing Raji and Ramos cell proliferation.

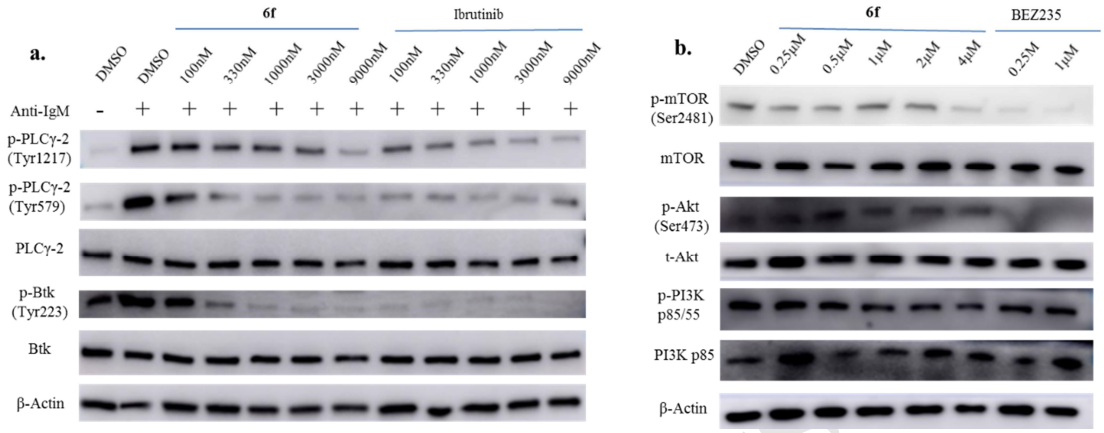

Figure 4 Effect of **6f** on BTK and PI3K mediated signaling pathway in the Ramos cell line

2.2.5 Effect of **6f** on cell apoptosis and cycle

In order to explore the anti-proliferative mechanism of **6f** on B-cell leukemia cells, the effect on apoptosis and on the cell cycle distribution of **6f** on Ramos cells was detected using flow cytometry analysis. As shown in Figure 5, BEZ235 treatment significantly induced Ramos cell apoptosis (Figure 5d) while ibrutinib treatment only leaded to slight apoptosis after 48h incubation (Figure 5b). Furthermore, **6f** induced signally apoptosis of Ramos cells (positive Annexin-V% was 89.7%) with the low dose of 5 μM (Figure 5c). Moreover, 6f could induce the growth arrest of Ramos cells at the G_0/G_1 phase compared with vehicle treatment. The G_0/G_1 phase arrest was also found with the treatment of ibrutinib or BEZ235.

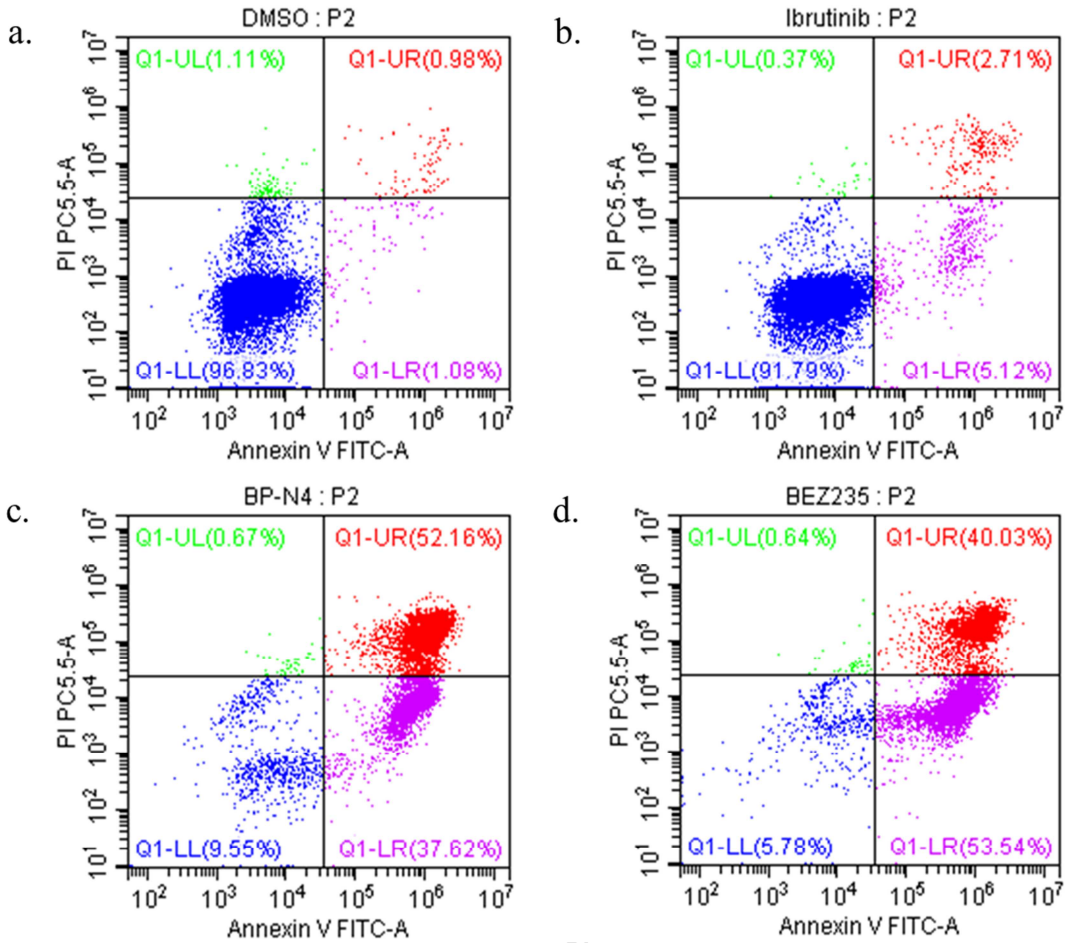

Figure 5. Compound **6f** induced Ramos cell apoptosis in vitro. The cells were incubated with compound **6f** (5 μM) for 48h, and the cells were stained with annexin V/FITC, followed by flow cytometry analysis.

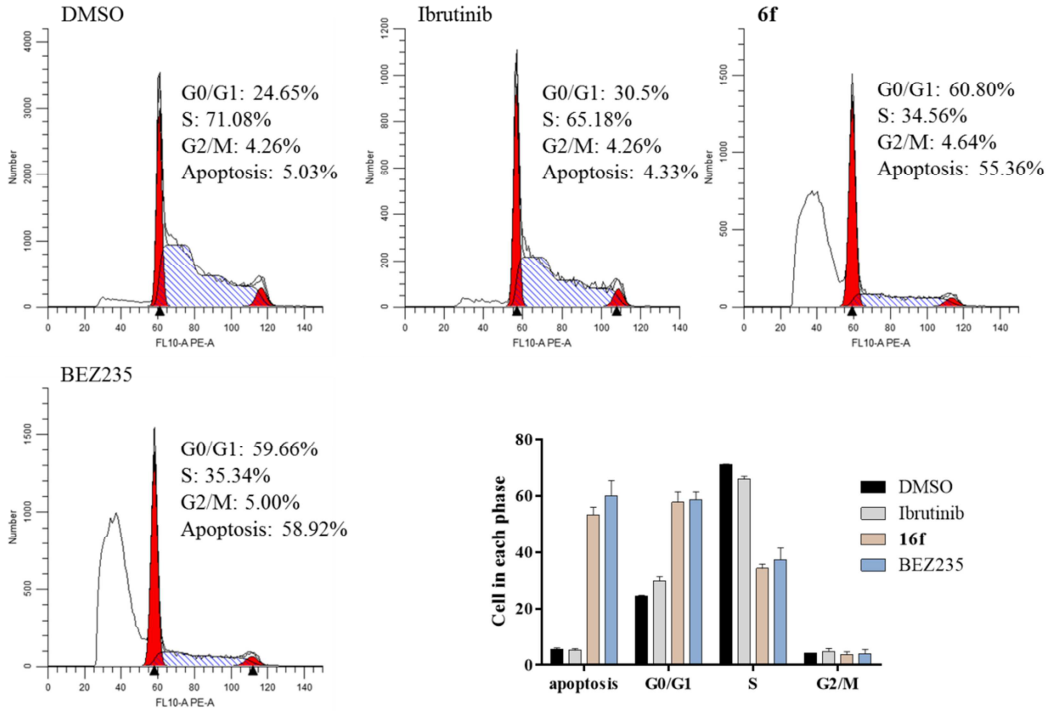

Figure 6. Effect of **6f** (5 μM) on Ramos cell cycle arrest detected by flow cytometry assay.

2.3 ADME properties study

Next, the preADMET server was used to predict ADME (Table 3). The calculated results show that the compound **6f** has good predicted solubility and better extracorporeal colon cancer cell permeability (caco-2) than that of BEZ235 and QL47, while human intestinal absorption is comparable and all values are greater than 97% [24]. All the data suggested that **6f** may have good predicted oral absorption and utilization. In addition, **6f** also showed good plasma protein binding rate (PPB, > 90%), but low BBB value (< 0.1), indicating that the compound has a long half-life and is less likely to be toxic to CNS. MDCK is an index to investigate the renal efflux of drugs, and the general value greater than 25 indicates better efflux [25,26]. From the predicted results, the three compounds showed no obvious efflux effect. In addition, preADMET provides information related to CYP450 metabolism. According to the results, **6f** is not a metabolic substrate of CYP_2D6 and CYP_3A4, which has better metabolic stability compared with BEZ235 and QL47. These data indicated that **6f** has better ADME properties than BEZ235 and QL47.

Table 3. Predicted ADME properties of BEZ235, QL47 and **6f**

SN	ADME properties	Compounds		
		BEZ235	QL47	**6f**
1	Water solubility in buffer system (SK atomic types, mg/L)	6.41	1.49	13.39
2	in vitro Caco-2 cell permeability (nm/sec)	27.82	38.77	42.64
3	Human intestinal absorption (HIA, %)	98.03	97.76	97.08
4	in vitro plasma protein binding (%)	93.83	98.22	94.47
5	in vivo blood-brain barrier penetration (C.brain/C.blood)	0.14	0.05	0.01
6	in vitro MDCK cell permeability (nm/sec)	0.04	0.08	0.39
7	CYP_2D6_substrate	Non	Non	Non
8	CYP_3A4_inhibition	Inhibitor	Inhibitor	Non
9	CYP_3A4_substrate	Substrate	Substrate	Non

2.4 Docking study

The biological studies above highlighted the utility of the newly synthesized benzofuro[3,2-*b*]pyridine-2(1*H*)-one derivatives as anti-leukemia agents. Thus, a molecular docking study was further performed in an attempt to gain some structural insights into their potential binding patterns and possible interactions with both BTK and PI3Kδ kinases. Accordingly, the most active derivative **6f** was docked inside the active sites of both BTK and PI3Kδ kinases. As shown in Figure 7a, it could be found that the furan oxygen atom of **6f** formed hydrogen bond with Met477 of BTK. Meanwhile, the acrylamide group formed covalent bonds with cysteine residue C481. Obviously, the covalent bond could significantly

increase the affinity of **6f** to BTK compared to **2**. In contrast to BTK, the inhibitory activity of **6f** against PI3Kδ was owed to the interaction of the pyridine with LYS799 and the lactam with SER831 (Figure 7b). Compared with **2**, the added interaction of lactam with SER831 improved the inhibitory activity of **6f** against PI3Kδ.

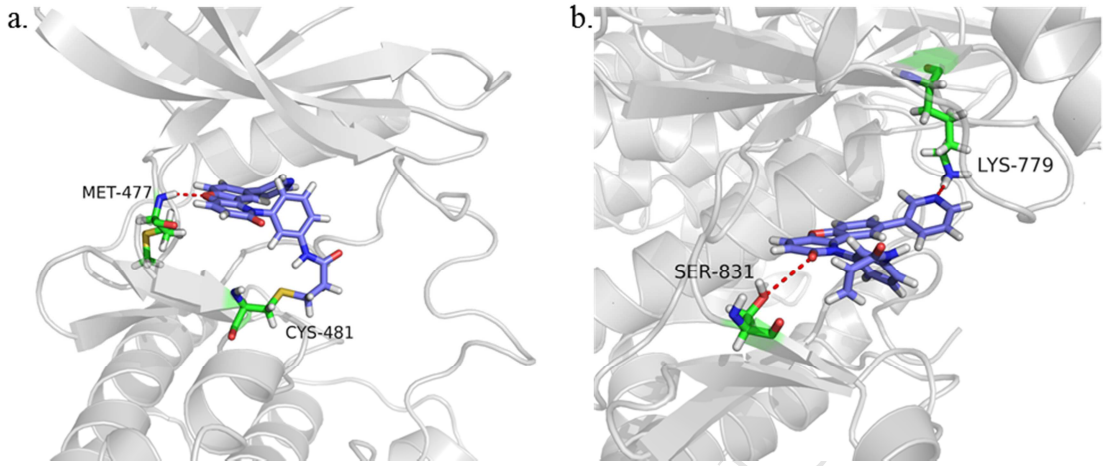

Figure 7. The docking model of **6f** with BTK (a, PDB: 3PIY) and PI3Kδ (b, 5O83)

3. Conclusion

In this study, a novel series of benzofuro[3,2-*b*]pyridin-2(1*H*)-one derivatives based on previous studies were synthesized and screened for their anticancer potential against two cancer cell lines at cellular level and two kinases at biochemical level. Among the newly synthesized analogs, compound **6f** exhibited the best dual BTK/PI3Kδ kinase inhibitory activity along with impressive anti-proliferative effects in Raji and Ramos leukemia cell lines. Additional studies identified **6f** significantly blocked the BCR/BTK pathway and PI3K/Akt/mTOR pathway. Moreover, **6f** also significantly arrested the cell cycle distribution and induced cell apoptosis. And the preADME server predicted the ADME properties of the obtained compound **6f**. The docking studies were performed to predict the possible binding patterns of the potent compound **6f** into the ATP-active sites of BTK and PI3Kδ kinases. Overall, we obtained a more potent compound **6f** based on the optimization of its derivative **2**. The docking simulation study, along with the in vitro assay results identified a promising duel BTK/ PI3Kδ inhibitor **6f** for the further development in the treatment of B-cell lymphoblastic leukemia.

4. Experimental protocols

4.1. Chemistry

Chemical reagents and solvents were obtained from commercial sources. Solvents were dried by standard methods when necessary. Reactions were monitored by thin-layer chromatography (TLC) using precoated silica gel plates (silica gel GF/UV 254), and spots were visualized under UV light (254 nm). Melting points (uncorrected) were determined on a Mel-TEMP II melting point apparatus and are uncorrected. ^{1}H-NMR and ^{13}C-NMR spectra were recorded with a Bruker Avance 300 MHz spectrometer at 300 MHz and 75 MHz, respectively in DMSO-d_6 or $CDCl_3$. MS spectra or high-resolution mass spectra (HRMS) were recorded on an Agilent 1946A-MSD (ESI)

Mass Spectrum or Agilent 6230 Series Accurate-Mass Time-Of-Flight (TOF) LC/MS. Chemical shifts were reported on the d scale and *J* values were given in Hz.

4.1.1 General procedures for the synthesis

4.1.1.1 General procedures A: Reduction of nitroarenes.

A suspension of nitroarene **S8** or **S20** in ethanol was heated at reflux. To this mixture was added iron (10 equiv) followed by a solution of NH_4Cl (10 equiv, 2.5 N) in H_2O. The resulting suspension was heated at reflux for 2 h. The hot mixture was then filtered through a Celite pad, and the filtrate was evaporated under vacuum. The residue was dissolved in EtOAc and washed with H_2O, and the aqueous phase was further extracted with ethyl acetate (2×20 mL). The organic extracts were combined, dried over Na_2SO_4, filtered, and evaporated under vacuum to obtain compounds **S9** or **S21**.

4.1.1.2 General procedures B: N-acetylation.

To a solution of arylamine in dimethylformamide at 0 °C was subsequently added K_2CO_3 (2 equiv), then dropwise added acyl chloride (1.2 equiv). The solution was stirred for 1 h at room temperature and quenched with H_2O (150 mL). The aqueous phase was further extracted with ethyl acetate (2×20 mL). The organic extracts were combined, dried over Na_2SO_4, filtered and concentrated, the residue was subjected to column purification (CH_2Cl_2/ MeOH) to furnish the desired compounds.

4.1.1.3 General procedures C: halide displacement by amine

To a solution of chloracetyl compounds in dimethylformamide was subsequently added K_2CO_3 (2 equiv) and KI (catalytic amount), then added the amine (5 equiv). The solution was stirred for 2 h at r.t. and quenched with H_2O (150 mL). The aqueous phase was further extracted with ethyl acetate (2×20 mL). The organic extracts were combined, dried over Na_2SO_4, filtered and concentrated, the residue was subjected to column purification (CH_2Cl_2/ MeOH) to furnish the desired compounds.

4.1.1.4 General procedures D: Suzuki coupling

To a solution of bromoaryl compounds in 1,4-dioxane at room temperature was subsequently added $PdCl_2(Ph_3P)_2$ (0.1 equiv), K_2CO_3(3 equiv), and boronic acids or pinacol boronate esters and a few drops of water. After degassing, the resulting mixture was heated to 80 °C for 4-12 h before cooling to room temperature and filtering through Celite. Upon removal of the solvents, the residue was subjected to column purification (CH_2Cl_2/ MeOH) to furnish the desired compounds.

4.1.2 The synthesis of series **5a~5f** compounds

4.1.2.1 5-bromo-N-(4-nitrophenyl)benzofuran-3-amine (**S6a**)

To a solution of compound **S5** (1.3 g, 6.1 mmol) in toluene was subsequently paranitroaniline

(0.9 g, 6.l mmol). The resulting suspension was heated at reflux for 2 h with and concentrated, then the resulting yellow precipitate was recovered by filtration. (yield: 100%, 2.03 g). ^{1}H-NMR (300MHz, d_6-DMSO): δ ppm 9.19 (s, 1H), 8.33 (s, 1H), 8.10 (d, J = 9.2 Hz, 2H), 7.89 (d, J = 1.95Hz,1H), 7.58 (d, J = 8.7 Hz, 1H), 7.52 (dd, J = 1.9, 8.7 Hz, 1H), 7.04 (d, J = 9.2 Hz, 2H).

4.1.2.2 N-(5-bromobenzofuran-3-yl)-N-(4-nitrophenyl)acetamide (**S7a**)

To a solution of compound **S6a** (0.4 g, 1.2 mmol) in dimethylformamide was subsequently added 60% sodium hydride (86 mg, 2.16 mmol) in batches at ice bath. Until there is no bubble, the acetylchloride (86 mg, 2.16 mmol) was dropped slowly into the reaction, then stirred 0.5h continually. The reaction mixture was poured into water and was further extracted with ethyl acetate. The organic extracts were combined, dried over Na_2SO_4, filtered, and evaporated under vacuum and was subjected to column purification (CH_2Cl_2/ MeOH) to furnish the desired compound **S7** (yield: 71%, 0.32 g), MS (ESI, m/z): 374 $[M+H]^+$.

4.1.2.3 8-bromo-1-(4-nitrophenyl)benzofuro[3,2-*b*]pyridin-2(1*H*)-one (**S8a**)

To dimethylformamide (2.8 ml, 36.6 mmol) was added phosphoryl chloride (3.4 ml, 36.6 mmol) slowly at ice bath. After finished, the reaction mixture stirred 0.5h continually. Then the **S7** (6.85 g, 18.3 mmol) in dimethylformamide was added into the reaction solution, which was subsequently heated at 90 °C for 2h. The reaction mixture was cooled and poured into water, further extracted with ethyl acetate. The organic extracts were combined, dried over Na_2SO_4, filtered, and evaporated under vacuum and was subjected to column purification (CH_2Cl_2/MeOH) to furnish the desired compound **S8** (yield: 35.5%, 2.5 g). ^{1}H-NMR (300MHz, d_6-DMSO): δ ppm 8.54 (d, J = 8.94 Hz, 2H), 8.22 (d, J = 9.87 Hz, 1H), 7.92 (d, J = 8.94 Hz, 2H), 7.76 (d, J = 8.91 Hz, 1H), 7.63 (dd, J = 1.74, 8.91 Hz, 1H), 6.72 (d, J = 9.87 Hz, 1H), 6.3 (d, J = 1.74 Hz, 1H).

4.1.2.4 8-bromo-1- (4-aminophenyl)-benzofuro [3,2-*b*]pyridin-2(1*H*)-one (**S9a**）

The preparation of **S9a** was from **S8a** according to the general procedure A, yellow solid (yield: 80%). ^{1}H-NMR (300 MHz, d_6-DMSO): δ ppm 8.09 (d, J = 9.8 Hz, 1H), 7.69 (d, J = 8.9 Hz, 1H), 7.58 (dd, J = 8.9, 2.0 Hz, 1H), 7.08 (d, J = 8.6 Hz, 2H), 6.78 (d, J = 8.6 Hz, 2H), 6.61 (d, J = 9.8 Hz, 1H), 6.39 (d, J = 1.9 Hz, 1H), 5.58 (s, 2H). MS (ESI, m/z), $[M+Na]^+$: 377.

4.3.5 N-(4-(8-bromo-2-oxobenzofuro[3,2-b]pyridin-1(2H)-yl)phenyl)-2-(dimethylamino)aceta–mide (**S12**)

The preparation of S12 was from S9a according to the general procedure A and B, yellow solid (yield: 70%). ^{1}H-NMR (300 MHz, d_6-DMSO): δ ppm 9.41 (s, 1H), 7.93 (d, J = 8.7Hz, 2H), 7.80 (d, J = 9.7 Hz, 1H), 7.47 (dd, J = 2.0, 8.9 Hz, 1H), 7.42 (d, J = 8.7 Hz, 2H), 6.75 (d, J = 9.7 Hz, 1H), 6.52 (d, J = 1.8 Hz, 1H), 3.16 (s, 3H), 2.44 (s, 6H).

4.1.2.5 1-(4-dimethylamino-acetamido-phenyl)-8-(4-indol)-benzofuro[3,2-*b*]pyridin-2(1*H*)-one (**5a**)

General procedure D, yellow solid (yield: 54%). M.p. 146-151 °C; ^{1}H-NMR (300 MHz, d_6-DMSO): δ ppm 11.21 (s, 1H), 9.93 (s, 1H), 8.12 (d, J = 9.7, 2H), 7.95 (d, J = 8.7 Hz, 2H), 7.78 (d, J = 8.6 Hz, 1H), 7.72 (dd, J = 1.6, 8.3 Hz, 1H), 7.48 (d, J =8.7 Hz, 2H), 7.29 (t, J = 2.7 Hz, 1H),

7.08 (t, *J*= 7.4 Hz, 1H), 6.92 (d, *J* = 6.9 Hz, 1H), 6.63 (s, 1H), 6.62 (d, *J* = 9.7 Hz, 1H), 6.18 (s, 1H), 3.11 (s, 2H), 2.29 (s, 6H). ^{13}C-NMR (75 MHz, d_6-DMSO): δ ppm 168.92, 161.05, 154.33, 139.69, 138.94, 136.27, 136.06, 132.46, 131.61, 129.32, 128.34, 128.14, 125.70, 125.03, 121.19, 120.19, 119.30, 118.76, 118.49, 112.77, 110.87, 99.94, 63.34, 45.31. MS (ESI, m/z): 424 $[M-H]^-$.

4.1.2.6 1-(4- dimethylamino-acetamido-phenyl)-8-(3-pyridinyl)-benzofuro[3,2-*b*]pyridin-2(1*H*)-one (**5b**)

General procedure D, yellow solid (yield: 70%). M.p. 196-200 °C; ^{1}H-NMR (300 MHz, d_6-DMSO): δ ppm 11.21 (s, 1H), 10.08 (s, 1H), 8.13 (d, J = 10.0 Hz, 1H), 7.93 (d, *J* = 8.1 Hz, 2H), 7.80 (m, 2H), 7.70 (m, 1H), 7.47 (d, *J* = 8.1 Hz, 2H), 7.40 (m, 2H), 6.62 (d, *J*= 9.7 Hz, 1H), 6.25 (s, 1H), 3.15 (s, 2H), 2.32 (s, 6H). ^{13}C-NMR (75 MHz, d_6-DMSO): δ ppm 168.67, 161.46, 155.51, 148.98, 147.73, 140.12, 139.69, 138.66, 134.39, 133.14, 132.85, 131.69, 131.59, 129.25, 128.73, 128.59, 127.30, 124.44, 121.18, 119.86, 118.43, 113.85, 63.92, 45.45. HRMS (ESI) m/z calcd for $C_{26}H_{22}N_4O_3$ $[M+H]^+$ 439.1770, found 439.1771.

4.1.2.7 1-(4-dimethylamino-acetamido-phenyl)-8-(4-hydroxyphenyl)-benzofuro[3,2-*b*]pyridin-2(1*H*)–one (**5c**)

General procedure D, yellow solid (yield: 70%). M.p. 276-280 °C; ^{1}H-NMR (300 MHz, d_6-DMSO): δ ppm 10.11 (s, 1H), 9.58 (s, 1H), 8.11 (d, *J* = 9.7 Hz, 1H), 7.96 (d, *J* = 8.2 Hz, 2H), 7.70 (d, *J* = 8.6 Hz, 1H), 7.64 (d, *J* = 9.2 Hz, 1H), 7.48 (d, *J* = 8.3 Hz, 2H), 7.12 (d, *J* = 8.1 Hz, 2H), 6.73 (d, *J* = 8.3 Hz, 2H), 6.61 (d, *J* = 9.8 Hz, 1H), 6.14 (s, 1H), 3.18 (s, 2H), 2.34 (s, 6H). ^{13}C-NMR (75 MHz, d_6-DMSO): δ ppm 169.06, 160.89, 157.04, 154.18, 139.60, 138.91, 135.50, 132.65, 130.03, 129.39, 128.64, 128.12, 127.43, 126.09, 120.58, 118.99, 118.79, 116.81, 115.71, 112.70, 63.37, 45.28. MS (ESI, m/z): 454 $[M+H]^+$.

4.1.2.8 1-(4-dimethylamino-acetamido-phenyl)-8-(4-N-t-butyloxycarboryl-piperidyl)-benzofuro [3,2-*b*]pyridin-2(1*H*)-one (**5d**)

General procedure D, yellow solid (yield: 74%). M.p. 155-160 °C; ^{1}H-NMR (300 MHz, d_6-DMSO): δ ppm 10.12 (s, 1H), 8.08 (d, *J* = 9.8 Hz, 1H), 7.96 (t, *J* = 11.2 Hz, 2H), 7.61 (d, *J* = 8.8 Hz, 1H), 7.53 (dd, *J* = 8.9, 1.6 Hz, 1H), 7.44 (d, *J* = 8.7 Hz, 2H), 6.59 (d, *J* = 9.8 Hz, 1H), 5.95 (s, 1H), 5.89 (s, 1H), 3.88 (s, 2H), 3.17 (s, 2H), 2.34 (s, 6H), 2.08 (s, 2H), 1.41 (s, 9H). ^{13}C-NMR (75 MHz, d_6-DMSO): δ ppm 168.97, 160.82, 154.40, 153.78, 139.52, 138.83, 134.97, 133.12, 132.63, 129.33, 128.59, 128.06, 124.67, 120.81, 118.77, 118.49, 115.57, 112.33, 78.84, 63.31, 54.85, 45.25, 28.04, 26.31. MS (ESI, m/z): 543$[M-H]^-$.

4.1.2.9 1-(4-dimethylamino-acetamido-phenyl)-8-(4-piperidyl)-benzofuro[3,2-*b*]pyridin-2(1*H*)-one (**5e**)

Compound **5c** was solved in DCM, trifluoroacetic acid was added dropwise in ice bath. Then

the reaction was stirred at 0 ℃ for 2h and was monitored by TLC to confirm its completion. The pH was adjusted to basicity with sodium carbonate, and the reaction mixture was extracted with ethyl acetate for twice. The organic extracts were combined, dried over Na_2SO_4, filtered, and evaporated under vacuum and was subjected to column purification (CH_2Cl_2/ MeOH) to furnish the desired compound (yield: 60%). M.p. 120-126 ℃; ^{1}H-NMR (300 MHz, d_6-DMSO): δ ppm 10.85 (s, 1H), 8.11 (d, J = 9.8 Hz, 1H), 7.90 (d, J = 8.6 Hz, 2H), 7.67 (t, J = 9.2 Hz, 1H), 7.60 (d, J = 8.8 Hz, 1H), 7.49 (d, J = 8.6 Hz, 2H), 6.61 (d, J = 9.8 Hz, 1H), 6.03 (s, 1H), 5.95 (s, 1H), 3.72 (s, 2H), 3.65 (s, 4H), 3.19 (d, J = 5.4 Hz, 2H), 2.58 (d, J = 24.4 Hz, 6H), 2.34 (s, 1H). ^{13}C-NMR (75 MHz, d_6-DMSO): δ ppm 166.57, 160.85, 154.65, 139.09, 139.01, 133.89, 133.08, 132.94, 129.13, 128.73, 128.19, 124.70, 121.30, 118.98, 118.52, 117.10, 115.70, 112.33, 78.84, 63.31, 45.35, 44.39, 41.20, 22.91. HRMS (ESI) m/z calcd for $C_{26}H_{28}N_4O_3$ $[M+H]^+$ 445.2240, found 445.2241.

4.1.2.10 1-(4-acryloylamino-phenyl)-8-(3-(6-fluopyridinyl))-benzofuro[3,2-*b*]pyridin-2(1*H*)-one (**5f**)

General procedure D, yellow solid (yield: 73%). M.p. 278-286 ℃; ^{1}H-NMR (300 MHz, d_6-DMSO): δ ppm 10.49 (s, 1H), 8.09 (t, J = 8.6 Hz, 2H), 7.89 (dd, J = 22.8, 8.1 Hz, 3H), 7.74 (dd, J = 16.2, 8.6 Hz, 2H), 7.47 (dd, J = 17.2, 8.4 Hz, 2H), 7.11 (d, J = 8.2 Hz, 1H), 6.62 (d, J = 9.8 Hz, 1H), 6.57 – 6.42 (m, 1H), 6.34 (d, J = 16.0 Hz, 1H), 6.21 (d, J = 15.8 Hz, 1H), 5.82 (d, J = 9.0 Hz, 1H). ^{13}C-NMR (75 MHz, d_6-DMSO): δ ppm 163.45, 160.88, 154.87, 144.89, 144.69, 139.84, 139.17, 133.53, 132.55, 131.57, 131.09, 128.84, 128.13, 127.54, 126.76, 120.49, 120.18, 119.34, 119.11, 117.79, 113.26, 109.96, 109.46. MS (ESI, m/z): 425 $[M+H]^+$.

4.1.3 The synthesis of series **6a~6g** compounds

4.1.3.1 1-(3-aminophenyl)-8-bromobenzofuro[3,2-*b*]pyridin-2(1H)-one (**S9b**)

The preparation of **S9b** was synthesized with the similar procedure of **S9a**, yellow solid (yield: 75%).^{1}H-NMR (300 MHz, d_6-DMSO): δ ppm 8.09 (d, J = 9.8 Hz, 1H), 7.69 (d, J = 8.9 Hz, 1H), 7.58 (dd, J = 8.9, 2.0 Hz, 1H), 7.32 (t, J = 7.9 Hz, 1H), 6.86 (t, J = 7.9 Hz, 1H), 6.75 – 6.54 (m, 2H), 6.43 (s, 1H), 6.39 (d, J = 1.9 Hz, 1H), 5.55 (s, 2H). MS (ESI, m/z), $[M+Na]^+$: 377.

4.1.3.2 8-(6-methoxypyridin-3-yl)-1-(3-aminophenyl)benzofuro[3,2-*b*]pyridin-2(1*H*)-one (**S14**)

General procedure D, yellow solid (yield: 81%). M.p. 271-274 ℃; ^{1}H-NMR (300 MHz, d_6-DMSO): δ ppm 8.20 – 8.03 (m, 1H), 7.74 (dd, J = 20.3, 8.8 Hz, 2H), 7.32 (t, J = 7.9 Hz, 1H), 6.86 (t, J = 7.9 Hz, 1H), 6.75 – 6.54 (m, 2H), 6.43 (s, 1H), 5.55 (s, 1H), 3.88 (s, 2H). ^{13}C-NMR (75 MHz, d_6-DMSO): δ ppm 163.44, 161.11, 155.06, 150.94, 144.60, 139.38, 138.81, 137.67, 132.66, 130.56, 129.44, 129.17, 128.33, 126.84, 119.57, 117.95, 114.88, 113.37, 111.14, 53.80. MS (ESI, m/z): 382 $[M-H]^-$.

4.1.3.3 8-(6-methoxypyridin-3-yl)-1-(3-(1-N-methyl-piperazinyl)-acetamido-phenyl)benzofuro

[3,2-*b*]pyridin-2(1*H*)-one (**6a**)

The preparation of **6a** was obtained for two steps according the general procedure B and C, yellow solid (yield: 71%). M.p. 225-230 °C; ^{1}H-NMR (300 MHz, d_6-DMSO): δ ppm 10.06 (s, 1H), 8.13 (d, *J* = 9.7 Hz, 1H), 8.04 (s, 1H), 7.95 (s, 1H), 7.88 (d, *J* = 8.1 Hz, 1H), 7.76 (d, *J* = 8.6 Hz, 1H), 7.72 – 7.58 (m, 3H), 7.26 (d, *J* = 7.1 Hz, 1H), 6.81 (d, *J* = 8.6 Hz, 1H), 6.64 (d, *J* = 9.7 Hz, 1H), 6.29 (s, 1H), 3.85 (s, 3H), 3.21 – 3.08 (m, 2H), 2.51 (s, 4H), 2.39 (s, 4H), 2.17 (s, 3H). ^{13}C-NMR (75 MHz, d_6-DMSO): δ ppm 169.29, 163.44, 161.16, 155.09, 144.67, 140.54, 139.61, 138.24, 137.72, 132.83, 130.62, 129.20, 129.11, 128.73, 127.03, 123.58, 120.62, 119.68, 119.51, 119.43, 117.69, 113.58, 111.15, 62.11, 54.72, 53.76, 52.79, 45.84. MS (ESI, m/z): 524 $[M+H]^+$.

4.1.3.4 8-(6-methoxypyridin-3-yl)-1-(3-dimethylamino-acetamido-phenyl)benzofuro[3,2-*b*] pyridin-2(1*H*)-one (**6b**)

The preparation of **6c** was obtained for two steps according the general procedure B and C, yellow solid (yield: 86%). M.p. 223-225 °C; ^{1}H-NMR (300 MHz, d_6-DMSO): δ ppm 10.09 (s, 1H), 8.16 (d, *J* = 10.1 Hz, 1H), 8.08 (s, 1H), 7.97 (s, 1H), 7.87 (d, *J* = 7.6 Hz, 1H), 7.81 (d, *J* = 9.0 Hz, 1H), 7.71 (d, *J* = 9.0 Hz, 1H), 7.64 (s, 2H), 7.28 (s, 1H), 6.84 (d, *J* = 8.3 Hz, 1H), 6.65 (d, *J* = 9.1 Hz, 1H), 6.32 (s, 1H), 3.86 (s, 3H), 3.09 (s, 2H), 2.25 (s, 6H). ^{13}C-NMR (75 MHz, d_6-DMSO): δ ppm 169.75, 163.40, 161.18, 155.05, 144.64, 140.66, 139.57, 138.17, 137.62, 132.74, 130.55, 129.12, 128.66, 126.91, 123.48, 120.66, 119.50, 117.66, 113.47, 111.05, 63.61, 53.72, 45.64. MS (ESI, m/z): 469 $[M+H]^+$.

4.1.3.5 8-(6-methoxypyridin-3-yl)-1-(3-(1-morpholinyl)-acetamido-phenyl)benzofuro[3,2-*b*] pyridin-2(1*H*)-one (**6c**)

The preparation of **6c** was obtained for two steps according the general procedure B and C, yellow solid (yield: 75%). M.p. 265-268 °C; ^{1}H-NMR (300 MHz, d_6-DMSO): δ ppm 10.06 (s, 1H), 8.16 (d, *J* = 9.7 Hz, 1H), 8.04 (s, 1H), 7.95 (s, 1H), 7.88 (d, *J* = 8.1 Hz, 1H), 7.76 (d, *J* = 8.6 Hz, 1H), 7.72 – 7.58 (m, 3H), 7.26 (d, *J* = 7.1 Hz, 1H), 6.81 (d, *J* = 8.6 Hz, 1H), 6.64 (d, *J* = 9.7 Hz, 1H), 6.29 (s, 1H), 3.86 (s, 3H), 3.59 (m, 4H), 3.14 (s, 2H), 2.39 (s, 4H). ^{13}C-NMR (75 MHz, d_6-DMSO): δ ppm 169.29, 163.11, 161.14, 155.11, 144.70, 140.51, 139.61, 138.24, 137.73, 132.83, 130.60, 129.21, 128.70, 127.01, 123.60, 120.67, 119.67, 117.69, 113.58, 111.15, 66.46, 62.51, 53.76, 53.58. MS (ESI, m/z): 533 $[M+Na]^+$.

4.1.3.6 8-(6-methoxypyridin-3-yl)-1-(3-amino-acetamido-phenyl)benzofuro[3,2-*b*]pyridin-2(1*H*)-one (**6d**)

The preparation of **6d** was obtained for two steps according the general procedure B and C, yellow solid (yield: 74%). M.p. 205-207 °C; ^{1}H-NMR (300 MHz, d_6-DMSO): δ ppm 8.11 (d, *J* = 9.8 Hz, 1H), 8.01 (s, 1H), 7.90 (s, 1H), 7.83 (d, *J* = 8.2 Hz, 1H), 7.74 (d, *J* = 8.7 Hz, 1H), 7.66 (d,

J = 7.6 Hz, 2H), 7.61 (dd, *J* = 6.4, 4.1 Hz, 1H), 7.25 (d, *J* = 7.7 Hz, 1H), 6.82 (d, *J* = 8.6 Hz, 1H), 6.61 (t, *J* = 8.6 Hz, 1H), 6.23 (s, 1H), 3.83 (s, 3H), 3.47 (s, 2H). ^{13}C-NMR (75 MHz, d_6-DMSO): δ ppm 170.01, 162.95, 160.70, 154.58, 144.14, 140.06, 139.13, 137.83, 137.31, 132.32, 130.29, 128.69, 128.59, 128.30, 126.58, 123.02, 119.84, 119.15, 118.89, 118.69, 117.04, 113.15, 110.75, 53.33, 43.93. MS (ESI, m/z): 441 $[M+H]^+$.

4.1.3.7 8-(6-methoxypyridin-3-yl)-1-(3-acrylamido-phenyl)benzofuro[3,2-*b*]pyridin-2(1*H*)-one (**6e**)

The preparation of **6e** was obtained for two steps according the general procedure B and D, yellow solid (yield: 74%). M.p. 290-295 °C; ^{1}H-NMR (300 MHz, d_6-DMSO): δ ppm 3.87 (s, 3H), 5.77 (d, *J* = 9.6 Hz, 1H), 6.26 (d, *J* = 16.3 Hz, 1H), 6.34 (s, 1H), 6.45 (dd, *J* = 10.1, 12.7 Hz, 1H), 6.65 (d, *J* = 9.5 Hz, 1H), 6.83 (d, *J* = 8.5 Hz, 1H), 7.31 (d, *J* = 7.89 Hz, 1H), 7.65 (d, *J* = 7.9 Hz, 2H), 7.72 (d, *J* = 8.6 Hz, 1H), 7.81 (m, 2H), 7.97 (s, 1H), 8.09 (s, 1H), 8.15 (d, *J*=9.51 Hz, 1H), 10.45 (s, 1H). ^{13}C-NMR (75 MHz, d_6-DMSO): δ ppm 164.02, 163.58, 161.19, 155.14, 152.07, 144.71, 144.04, 140.87, 139.69, 138.33, 137.81, 132.91, 131.97, 130.75, 128.80, 127.97, 127.11, 123.71, 120.58, 119.73, 119.53, 117.68, 114.63, 113.67, 111.19, 53.82. MS (ESI, m/z): 460 $[M+Na]^+$.

4.1.3.8 1-(3-acryloylamino-phenyl)-8-(3-pyridinyl)-benzofuro[3,2-*b*]pyridin-2(1*H*)-one (**6f**)

The preparation of **6f** was obtained for two steps according the general procedure B and D, yellow solid (yield: 80%). M.p. 294-296 °C; ^{1}H-NMR (300 MHz, d_6-DMSO): δ ppm 10.57 (s, 1H), 8.49 (s, 2H), 8.17 (d, *J* = 9.9 Hz, 1H), 8.01 (s, 1H), 7.81 (d, *J* = 8.4 Hz, 3H), 7.69 (dd, *J* = 18.8, 8.1 Hz, 2H), 7.40 (s, 1H), 7.31 (d, *J* = 7.2 Hz, 1H), 6.67 (d, *J* = 9.7 Hz, 1H), 6.45 (dd, *J* = 16.6, 10.5 Hz, 1H), 6.37 (s, 1H), 6.25 (d, *J* = 16.9 Hz, 1H), 5.77 (d, *J* = 10.6 Hz, 1H). ^{13}C-NMR (75 MHz, d_6-DMSO): δ ppm 163.51, 160.67, 154.96, 148.47, 147.17, 140.40, 139.24, 137.79, 134.99, 133.91, 132.40, 131.43, 130.31, 128.59, 128.34, 127.54, 126.95, 123.89, 123.22, 120.08, 119.37, 118.98, 117.92, 113.35. MS (ESI, m/z): 406 $[M-H]^-$.

4.1.3.9 1-(3-acryloylamino-phenyl)-8-(3-(6-fluo-pyridinyl))-benzofuro[3,2-*b*]pyridin-2(1*H*)-one (**6g**)

The preparation of **6g** was obtained for two steps according the general procedure B and D, yellow solid (yield: 76%). M.p. 281-286 °C; ^{1}H-NMR (300 MHz, d_6-DMSO): δ ppm 10.45 (s, 1H), 8.09 (d, *J* = 1.3 Hz 1H), 8.07 (s, 1H), 7.85 (m, 2H), 7.75 (m, 3H), 7.56 (m, 1H), 7.19 (d, *J* = 6.3 Hz 1H), 7.11 (d, *J* = 5.9 Hz, 1H), 6.57 (d, *J* = 1.3 Hz, 1H), 6.28 (m, 1H), 6.22 (s, 1H), 6.13 (),d, *J* = 16.92, 1H), 5.66 (d, *J* = 9.84 Hz, 1H). ^{13}C-NMR (75 MHz, d_6-DMSO): δ ppm 163.49, 160.65, 154.96, 144.96, 144.75, 140.17, 139.27, 137.74, 131.40, 131.25, 130.70, 130.31, 128.74, 128.35, 127.59, 126.99, 123.25, 120.15, 119.45, 119.06, 117.95, 113.37, 110.10, 109.61. MS (ESI, m/z):

425 $[M+H]^+$.

4.1.4 The synthesis of series **7a~7d** compounds

4.1.4.1 5-bromo-N-(4-nitrophenyl)furo[2,3-*b*]pyridin-3-amine (**S18**)

To a solution of compound **S17** (4.3 g, 20.2 mmol) in toluene was subsequently paranitroaniline (2.8 g, 20.2 mmol). The resulting suspension was heated at reflux for 2 h with and concentrated, then the resulting yellow precipitate was recovered by filtration. (yield: 92%, 6.2 g). ^{1}H-NMR (300 MHz, d_6-DMSO): δ ppm 7.06 (d, J = 9.2 Hz, 2H), 8.12 (d, J=9.2 Hz, 2H), 8.4 (d, J = 2.2 Hz, 1H), 8.43 (s, 1H), 8.46 (d, J = 2.2 Hz, 1H), 9.29 (s, 1H).

4.1.4.2 N-(5-bromofuro[2,3-*b*]pyridin-3-yl)-N-(4-nitrophenyl)acetamide (**S19**)

To a solution of compound **S18** (6.24 g, 18.68 mmol) in dimethylformamide was subsequently added 60% sodium hydride (1.12 g, 28 mmol) in batches at ice bath. Until there is no bubble, the acetylchloride (2 ml, 28 mmol) was dropped slowly into the reaction, then stirred 0.5h continually. The reaction mixture was poured into water, filtered and dried on infrared. The solid was used without further purified.

4.1.4.3 8-bromo-1-(4- nitrophenyl)furo[2,3-*b*:4,5-*b'*]dipyridin-2(1*H*)-one (**S20**)

To dimethylformamide (2.8 ml, 36.6 mmol) was added phosphoryl chloride (3.4 ml, 36.6 mmol) slowly at ice bath. After finished, the reaction mixture stirred 0.5h continually. Then the **S19** (6.85 g, 18.3 mmol) in dimethylformamide was added into the reaction solution, which was subsequently heated at 90 °C for 3h. The reaction mixture was cooled and poured into water, further extracted with ethyl acetate. The organic extracts were combined, dried over Na_2SO_4, filtered, and evaporated under vacuum and was subjected to column purification (CH_2Cl_2/ MeOH) to furnish the desired compound **S20** (yield: 35.5%, 2.5 g). ^{1}H-NMR (300 MHz, d_6-DMSO): δ ppm 6.75 (d, J = 9.8 Hz, 1H), 6.82 (d, J = 2.2 Hz, 1H), 7.86 (d, J = 8.9 Hz, 2H), 8.22 (d, J = 9.8 Hz, 1H), 8.49 (d, J = 8.9 Hz, 2H), 8.51 (d, J = 2.2 Hz, 1H).

4.1.4.4 1-(4-aminophenyl)-8-bromofuro[2,3-*b*:4,5-*b'*]dipyridin-2(1H)-one (**S21**)

The preparation of **S21** was from **S20** according to the general procedure A，yellow solid (yield: 86%). ^{1}H-NMR (300 MHz, d_6-DMSO): δ ppm 8.51 (d, J = 2.1 Hz, 1H), 8.22 (d, J = 9.8 Hz, 1H), 7.08 (d, J = 8.6 Hz, 2H), 6.82 (d, J = 2.1 Hz, 1H), 6.78 (d, J = 8.6 Hz, 2H), 6.75 (d, J = 9.8 Hz, 1H).

4.1.4.5 1-(4-aminophenyl)-8-(6-methoxypyridin-3-yl)furo[2,3-*b*:4,5-*b'*]dipyridin-2(1H)-one (**S22**)

General procedure D, yellow solid (yield: 86%). ^{1}H-NMR (300 MHz, d_6-DMSO): δ ppm 3.98 (s, 3H), 5.55 (s, 2H), 6.67 (d, J = 9.7 Hz, 1H), 6.78 (s, 1H), 6.79 (d, J = 9.0 Hz, 2H), 6.91 (d, J = 8.6 Hz, 1H), 7.14 (d, J = 9.0 Hz, 2H), 7.79 (dd, J = 2.5, 8.6 Hz, 1H), 8.13 (d, J = 9.7 Hz, 1H), 8.17 (d, J = 2.2 Hz, 1H), 8.65 (d, J = 2.2 Hz,1H).

4.1.4.6 2-(dimethylamino)-N-(4-(8-(6-methoxypyridin-3-yl)-2-methylenefuro[2,3-*b*:4,5-*b'*]

dipyridin-1(2*H*)-yl)phenyl)acetamide (**7a**)

The preparation of **7a** was obtained for two steps according the general procedure B and C, yellow solid (yield: 70%). M.p. 210-215 °C; ^{1}H-NMR (300 MHz, d_6-DMSO): δ ppm 9.42 (s, 1H), 8.50 (s, 1H), 8.11 (s, 1H), 7.90 (t, *J* = 9.6 Hz, 3H), 7.55 (dt, *J* = 11.2, 5.6 Hz, 1H), 7.45 (t, *J* = 8.9 Hz, 2H), 6.82 (dd, *J* = 8.9, 6.8 Hz, 3H), 3.94 (s, 3H), 3.15 (s, 2H), 2.42 (s, 6H). ^{13}C-NMR (75 MHz, d_6-DMSO): δ ppm 169.26, 164.06, 161.83, 160.88, 145.55, 145.07, 139.24, 138.63, 137.51, 132.50, 130.38, 128.53, 127.88, 127.23, 126.29, 121.44, 120.63, 112.00, 111.44, 63.65, 53.68, 46.06. HRMS (ESI) m/z calcd for $C_{26}H_{23}N_5O_4$ $[M+H]^+$ 470.1828, found 470.1824.

4.1.4.7 N-(4-(8-(6-methoxypyridin-3-yl)-2-oxofuro[2,3-*b*:4,5-*b'*]dipyridin-1(2H)-yl)phenyl)-2-(piperazin-1-yl)acetamide (**7b**)

The preparation of **7b** was obtained for two steps according the general procedure B and C, yellow solid (yield: 40%). M.p. 195-198 °C; ^{1}H-NMR (300 MHz, d_6-DMSO): δ ppm 2.31 (brs, 4H), 2.49 (brs, 4H), 3.23 (s, 2H), 3.85 (s, 3H), 6.57 (s, 1H), 6.79 (d, *J* = 9.8 Hz, 1H), 6.83 (d, *J* = 8.6 Hz, 1H), 7.51 (d, *J* = 8.5 Hz, 2H), 7.68 (dd, *J* = 2.2, 8.58 Hz, 1H), 7.93 (d, *J* = 8.6 Hz, 2H), 8.13 (s, 1H), 8.15 (d, *J* = 9.9 Hz, 1H), 8.63 (d, *J* = 1.9 Hz, 1H), 10.11 (s, 1H). ^{13}C-NMR (75 MHz, d_6-DMSO): δ ppm 168.68, 163.37, 160.61, 160.23, 154.72, 154.21, 145.11, 144.62, 139.58, 137.81, 137.48, 132.14, 129.23, 128.52, 128.22, 127.63, 126.28, 125.79, 120.84, 120.52, 111.46, 110.92, 107.23, 61.57, 54.21, 53.34, 52.17, 45.43. HRMS (ESI) m/z calcd for $C_{28}H_{26}N_6O_4$ $[M+H]^+$ 511.2094, found 511.2092.

4.1.4.8 N-(4-(8-(6-methoxypyridin-3-yl)-2-oxofuro[2,3-*b*:4,5-*b'*]dipyridin-1(2H)-yl)phenyl)-2-(piperidin-1-yl)acetamide (**7c**)

The preparation of **7c** was obtained for two steps according the general procedure B and C, yellow solid (yield: 65%). M.p. 178-182 °C; ^{1}H-NMR (300 MHz, d_6-DMSO): δ ppm 9.57 (s, 1H), 8.49 (d, *J* = 2.1 Hz, 1H), 8.10 (d, *J* = 2.3 Hz, 1H), 7.89 (d, *J* = 4.3 Hz, 1H), 7.86 (d, *J* = 5.4 Hz, 2H), 7.55 (dd, *J* = 8.6, 2.5 Hz, 1H), 7.46 (d, *J* = 8.7 Hz, 2H), 6.87 – 6.81 (m, 1H), 6.80 (d, *J* = 3.9 Hz, 1H), 6.78 (s, 1H), 3.92 (s, 3H), 3.13 (s, 2H), 2.57 (d, *J* = 4.7 Hz, 4H), 1.83 – 1.56 (m, 4H), 1.51 (d, *J* = 4.6 Hz, 2H). ^{13}C-NMR (75 MHz, d_6-DMSO): δ ppm 169.58, 163.84, 161.10, 160.71, 145.59, 145.09, 140.08, 138.29, 137.94, 137.52, 132.61, 129.69, 129.01, 128.86, 128.71, 128.12, 126.73, 126.25, 121.33, 120.99, 120.80, 111.94, 111.38, 100.50, 63.19, 54.51, 53.81, 25.87, 24.02. HRMS (ESI) m/z calcd for $C_{29}H_{27}N_5O_4$ $[M+H]^+$ 510.2141, found 510.2140.

4.1.4.9 N-(4-(2-oxo-8-(pyridin-3-yl)furo[2,3-*b*:4,5-*b'*]dipyridin-1(2H)-yl)phenyl)acrylamide (**7d**)

The preparation of **7d** was obtained for two steps according the general procedure B and D, yellow solid (yield: 65%). M.p. 256-260 °C; ^{1}H-NMR (300 MHz, d_6-DMSO): δ ppm 10.52 (s, 1H), 8.74 (s, 1H), 8.58 (s, 2H), 8.20 (d, *J* = 9.8 Hz, 1H), 7.95 (d, *J* = 8.6 Hz, 2H), 7.84 (d, *J* = 7.7 Hz,

1H), 7.56 (d, *J* = 8.6 Hz, 2H), 7.49 – 7.38 (m, 1H), 6.74 (d, *J* = 9.7 Hz, 1H), 6.72 (s, 1H), 6.50 (dd, *J* = 16.9, 9.9 Hz, 1H), 6.33 (d, *J* = 17.1 Hz, 1H), 5.83 (d, *J* = 10.2 Hz, 1H). ^{13}C-NMR (75 MHz, d_6-DMSO): δ ppm 163.44, 160.64, 149.16, 147.37, 145.62, 139.93, 137.94, 134.30, 132.25, 132.16, 131.55, 129.30, 128.68, 128.29, 127.58, 127.05, 124.03, 121.01, 120.43, 111.58. MS (ESI, m/z): 407 $[M-H]^-$.

4.2 Biological screening

4.2.1. Cell culture

The human cell lines Raji (Burkitt lymphoma cell line), Ramos cells (Burkitt lymphoma cell line cell line) were obtained from Chinese academy of sciences cell bank. Cancer cell lines were maintained as a monolayer culture in PRAM1640 or IMDM (Keygentech, CN), supplemented with 10% FBS (Gibco) in a humidified atmosphere (5% CO_2) at 37°C.

4.2.2. Antiproliferative assays

Cellular chemo-sensitivity was determined by using a modified CCK-8 (Dojindo) method assay in vitro. In brief, Raji and Ramos cells in 200 ml culture medium were seeded into 96-well microplates at 3000-5000 cells per well respectively and cultured in PRAM1640 or IMDM with 10% FBS, incubated at 37 °C for 12-24 h prior to drug exposure. Cell numbers were titrated to keep control cells growing in the exponential phase throughout the 48 h incubation period. Cells were treated with several concentrations of tested compounds simultaneously and incubated for 48 h and then 10 ml of CCK-8 was added to each well and incubated for 4 h. The optical density at 450 nm was determined by Varioskan Flash Multimode Reader. The IC_{50} value, that is, the concentration (μM) of a compound was able to cause 50% cell death with respect to the control culture, was calculated according to the inhibition ratios. For temporal dependence of Raji cells viability, cells were collected at different time, then determined the cell viability with CCK-8.

4.2.3 In vitro kinase enzymatic assay

The BTK kinase enzyme assay system (Catalog: V9071, Promega, PI3K-Glo™ Class I Profiling Kit (Promega) and mTOR Lance Ultra Assay were used in this test. Concentrations consisting of suitable 200 nM were used for all of the tested compounds and 1nM~5μM were used for part of the tested compounds. The experiments were performed according to the instructions of the manufacturer. Measure the luminescence with a plate-reading luminometer or charge-coupled device (CCD) camera.

4.2.4 Western Blot

Cells was treatment with compounds for 4h, then stimulated with or not anti-human IgM F(ab')2 (Jackson Immuno Research Laboratories), and collected celles were washed twice with PBS, then collected and lysed in lysis buffer (100 mM of Tris–Cl, pH 6.8, 4% (m/v) SDS, 20% (v/v) glycerol, 200 mM of β-mercaptoethanol, 1mM of PMSF, 0.1 mM NaF and DTT) for 0.5 h on the ice. Heat sample to 95–100°C for 5 min; then cool on ice for 5 min; for 3 times. Protein concentration in the supernatants was detected by BCA protein assay (Thermo, Waltham, MA). Then equal amount of protein was separated with 12% SDS-PAGE and transferred to polyvinylidene difluoride (PVDF) membranes

(Millipore, Bedford, MA) using a semi-dry transfer system (Bio-rad, Hercules, CA). Proteins were detected using specific antibodies overnight at 4 °C followed by HRP-conjugated secondary antibodies for 1 h at 37 °C. All of the antibodies were diluted in PBST containing 1% BSA. Enhanced chemi-luminescent reagents (Beyotime, Jiangsu, China) were used to detect the HRP on the immunoblots, and the visualized bands were captured by film.

4.2.5 Flow cytometry assay

The Ramos cells (1 to 5 $\times 10^5$ cells/well) incubated in 6-well plates were treated with solvent control (DMSO), BEZ235, ibrutinib, or compound 6f in medium containing 5% FBS for 48 h. Then, collected and fixed with 70% ethanol at 4 °C overnight. After being fixed with 75% ethanol at 4 °C for 24 h, the cells were stained with Annexin V-FITC (5 μL)/propidium iodide (5 μL), and analyzed by flow cytometry assay (Becman Coulter, USA). For cell cycle analysis, Ramos cells at a density of approximately 1×10^6 cells/well were incubated in 6-well plates, treated with different concentrations of inhibitors for 48 h, collected and fixed with 70% ethanol at 4 °C overnight. After fixation, the cells were washed with PBS and stained with propidium iodide (PI) for 10 min under subdued light. Stained cells were analyzed flow cytometry assay (Becman Coulter, USA), and the results were performed using FCS Express flow cytometry analysis software (ModFit LT 3.1).

4.3 Docking study

The docking study was used with the CDOCKER model of Discovery Studio 3.0. The general step was step by step according to the course of Discovery Studio software. At last, the docking results were presented with Discovery Studio visualization.

For the in silico prediction, the PreADMET server application was used. The PreADMET approach is based on different classes of molecular parameters which are considered for generating quantitative structure properties.

Acknowledgement

We are grateful to the Program of Jiangsu Key Laboratory of Drug Design and Optimization, China Pharmaceutical University, postgraduate innovation fund of Huahai medical corporation and National Fund for Fostering talents of Basic Science for the financial support of this research.

References

[1] F. Melchers, Checkpoints that control B cell development, J Clin Invest. 125 (2015) 2203-2210.

[2] R.C. Rickert, New insights into pre-BCR and BCR signalling with relevance to B cell malignancies, Nat Rev Immunol. 13 (2013) 578-591.

[3] J.A. Burger, A. Wiestner, Targeting B cell receptor signalling in cancer: preclinical and clinical advances, Nat. Rev. Cancer. 18 (2018) 148-167.

[4] K. Bojarczuk, M. Bobrowicz, M. Dwojak, N. Miazek, P. Zapala, A. Bunes, M. Siernicka, M. Rozanska, M. Winiarska, B-cell receptor signaling in the pathogenesis of lymphoid malignancies, Blood Cell Mol. Dis. 55 (2015) 255-265.

[5] J.A. Burger, A. Wiestner, Targeting B cell receptor signalling in cancer: preclinical and clinical advances, Nat. Rev. Cancer. 18 (2018) 148-167.

[6] S.P. Treon, C.K. Tripsas, K. Meid, D. Warren, G. Varma, R. Green, K.V. Argyropoulos, G. Yang, Y. Cao, L. Xu, C.J. Patterson, S. Rodig, J.L. Zehnder, J.C. Aster, N.L. Harris, S. Kanan, I. Ghobrial, J.J. Castillo, J.P. Laubach, Z.R. Hunter, Z. Salman, J.L. Li, M. Cheng, F. Clow, T. Graef, M.L. Palomba, R.H. Advani, Ibrutinib in Previously Treated Waldenstrom's Macroglobulinemia, New Engl. J. Med. 372 (2015) 1430-1440.

[7] J.C. Byrd, B. Harrington, S. O'Brien, J.A. Jones, A. Schuh, S. Devereux, J. Chaves, W.G. Wierda, F.T. Awan, J.R. Brown, P. Hillmen, D.M. Stephens, P. Ghia, J.C. Barrientos, J.M. Pagel, J. Woyach, D. Johnson, J. Huang, X. Wang, A. Kaptein, B.J. Lannutti, T. Covey, M. Fardis, J. McGreivy, A. Hamdy, W. Rothbaum, R. Izumi, T.G. Diacovo, A.J. Johnson, R.R. Furman, Acalabrutinib (ACP-196) in Relapsed Chronic Lymphocytic Leukemia, New Engl. J. Med. 374 (2016) 323-332.

[8] K.S. Nair, B. Cheson, The role of idelalisib in the treatment of relapsed and refractory chronic lymphocytic leukemia, Ther. Adv. Hematol. 7 (2016) 69-84.

[9] A. Markham, Copanlisib: First Global Approval, Drugs. 77 (2017) 2057-2062.

[10] J.A. Woyach, R.R. Furman, T.M. Liu, H.G. Ozer, M. Zapatka, A.S. Ruppert, L. Xue, D.H. Li, S.M. Steggerda, M. Versele, S.S. Dave, J. Zhang, A.S. Yilmaz, S.M. Jaglowski, K.A. Blum, A. Lozanski, G. Lozanski, D.F. James, J.C. Barrientos, P. Lichter, S. Stilgenbauer, J.J. Buggy, B.Y. Chang, A.J. Johnson, J.C. Byrd, Resistance mechanisms for the Bruton's tyrosine kinase inhibitor ibrutinib, New Engl. J. Med. 370 (2014) 2286-2294.

[11] G. Salles, S.J. Schuster, S. de Vos, N.D. Wagner-Johnston, A. Viardot, K.A. Blum, C.R. Flowers, W.J. Jurczak, I.W. Flinn, B.S. Kahl, P. Martin, Y. Kim, S. Shreay, M. Will, B. Sorensen, M. Breuleux, P.L. Zinzani, A.K. Gopal, Efficacy and safety of idelalisib in patients with relapsed, rituximab- and alkylating agent-refractory follicular lymphoma: a subgroup analysis of a phase 2 study, Haematologica. 102 (2017) e156-e159.

[12] R. Morphy, Z. Rankovic, Designed multiple ligands. An emerging drug discovery paradigm, J. Med. Chem. 48 (2005) 6523-6543.

[13] N.M. O'Boyle, M.J. Meegan, Designed multiple ligands for cancer therapy, Curr. Med. Chem. 18 (2011) 4722-4737.

[14] J.D. Cooney, A.P. Lin, D.F. Jiang, L. Wang, A.N. Suhasini, J. Myers, Z.J. Qiu, A. Wolfler, H. Sill, R.C.T. Aguiar, Synergistic Targeting of the Regulatory and Catalytic Subunits of PI3K delta in Mature B-cell Malignancies, Clin. Cancer Res. 24 (2018) 1103-1113.

[15] M.F.M. de Rooij, A. Kuil, A.P. Kater, M.J. Kersten, S.T. Pals, M. Spaargaren, Ibrutinib and idelalisib synergistically target BCR-controlled adhesion in MCL and CLL: a rationale for combination therapy, Blood. 125 (2015) 2306-2308.

[16] S. Vakkalanka, K.V. Penmetsa, D. Chasse, Y.W. Chen, S. Viswanadha, D.R. Friedman, J.B. Weinberg, The dual PI3K delta/gamma inhibitor, RP6530, in combination with ibrutinib or fludarabine, synergistically enhances cytotoxicity in primary CLL cells in vitro., Clin. Cancer Res. 21 (2015).

[17] K. White, E. Murphy, K. Faia, J. Proctor, N. Kosmider, M. Pink, S. Goldstein, K. McGovern, J.L. Kutok, Combination of duvelisib with either ibrutinib or dexamethasone prevents mTOR-dependent feedback in aggressive B-cell lymphoma cell lines, Cancer Res. 76 (2016).

[18] A. Yahiaoui, S.A. Meadows, R.A. Sorensen, Z.H. Cui, K.S. Keegan, R. Brockett, G. Chen, C. Queva, L. Li, S.L. Tannheimer, PI3K delta inhibitor idelalisib in combination

with BTK inhibitor ONO/GS-4059 in diffuse large B cell lymphoma with acquired resistance to PI3K delta and BTK inhibitors, Plos One. 12 (2017).

[19] B. Pujala, A.K. Agarwal, S. Middya, M. Banerjee, A. Surya, A.K. Nayak, A. Gupta, S. Khare, R. Guguloth, N.A. Randive, B.U. Shinde, A. Thakur, D.I. Patel, M. Raja, M.J. Green, J. Alfaro, P. Avila, F.P. de Arce, R.G. Almirez, S. Kanno, S. Bernales, D.T. Hung, S. Chakravarty, E. McCullagh, K.P. Quinn, R. Rai, S.M. Pham, Discovery of Pyrazolopyrimidine Derivatives as Novel Dual Inhibitors of BTK and PI3K delta, ACS. Med. Chem. Lett. 7 (2016) 1161-1166.

[20] J. Alfaro, F.P. de Arce, S. Belmar, G. Fuentealba, P. Avila, G. Ureta, C. Flores, C. Acuna, L. Delgado, D. Gaete, B. Pujala, A. Barde, A.K. Nayak, T.V.R. Upendra, D. Patel, S. Chauhan, V.K. Sharma, S. Kanno, R.G. Almirez, D.T. Hung, S. Chakravarty, R. Rai, S. Bernales, K.P. Quinn, S.M. Pham, E. McCullagh, Dual Inhibition of Bruton's Tyrosine Kinase and Phosphoinositide-3-Kinase p110 delta as a Therapeutic Approach to Treat Non-Hodgkin's B Cell Malignanciess, J. Pharmacol. Exp. Ther. 361 (2017) 312-321.

[21] L.Y. Liu, B.Y. Shi, X.Y. Li, X.Q. Wang, X. Lu, X.R. Cai, A. Huang, G.S. Luo, Q.D. You, H. Xiang, Design and synthesis of benzofuro[3,2-b]pyridin-2(1H)-one derivatives as anti-leukemia agents by inhibiting BTK and PI3K delta, Bioorg. Med. Chem. 26 (2018) 4537-4543.

[22] H. Wu, W.C. Wang, F.Y. Liu, E.L. Weisberg, B. Tian, Y.F. Chen, B.H. Li, A.L. Wang, B.L. Wang, Z. Zhao, D.W. McMillin, C. Hu, H. Li, J.H. Wang, Y.K. Liang, S.J. Buhrlage, J.T. Liang, J. Liu, G. Yang, J.R. Brown, S.P. Treon, C.S. Mitsiades, J.D. Griffin, Q.S. Liu, N.S. Gray, Discovery of a Potent, Covalent BTK Inhibitor for B-Cell Lymphoma, ACS. Chem. Biol. 9 (2014) 1086-1091.

[23] S.M. Maira, F. Stauffer, J. Brueggen, P. Furet, C. Schnell, C. Fritsch, S. Brachmann, P. Chene, A. De Pover, K. Schoemaker, D. Fabbro, D. Gabriel, M. Simonen, L. Murphy, P. Finan, W. Sellers, C. Garcia-Echeverria, Identification and characterization of NVP-BEZ235, a new orally available dual phosphatidylinositol 3-kinase/mammalian target of rapamycin inhibitor with potent in vivo antitumor activity, Mol. Cancer Ther. 7 (2008) 1851-1863.

[24] S. Yee, In vitro permeability across Caco-2 cells (colonic) can predict in vivo (small intestinal) absorption in man--fact or myth, Pharm. Res. 14 (1997) 763-766.

[25] C.M. Nisha, A. Kumar, A. Vimal, B.M. Bai, D. Pal, A. Kumar, Docking and ADMET prediction of few GSK-3 inhibitors divulges 6-bromoindirubin-3-oxime as a potential inhibitor, J. Mol. Graph. Model. 65 (2016) 100-107.

[26] G. Jose, T.H. Suresha Kumara, H.B.V. Sowmya, D. Sriram, T.N. Guru Row, A.A. Hosamani, S.S. More, B. Janardhan, B.G. Harish, S. Telkar, Y.S. Ravikumar, Synthesis, molecular docking, antimycobacterial and antimicrobial evaluation of new pyrrolo[3,2-c]pyridine Mannich bases, Eur. J. Med. Chem. 131 (2017) 275-288.

- Simultaneously inhibiting BTK and PI3Kδ benefit of the treatment of leukemia
- A series of new benzofuro[3,2-*b*]pyridine-2(*1H*)-one derivatives were optimized from hit BTK/PI3Kδ inhibitor
- **6f** exhibited anti-leukemia activity by selectively inhibiting BTK kinase and PI3Kδ kinase